

Modeling Solar Irradiance for Short-term Dynamic Analysis of Power Systems

Guðrún Margrét Jónsdóttir, *Student Member, IEEE* and Federico Milano, *Fellow, IEEE*
 School of Electrical & Electronic Engineering, University College Dublin, Ireland
 gudrun.jonsdottir@ucdconnect.ie, federico.milano@ucd.ie

Abstract—This paper presents and compares four solar irradiance models for short-term power system analysis. Three of these models can be found in the literature but are based on approximations and shortcomings, which are duly discussed. The fourth model is novel and is formulated through stochastic differential equations with jumps. The case study illustrates the ability of the proposed solar irradiance model to generate synthetic processes that reproduce the stochastic properties of flickering events taken from measurement data.

Index Terms—Solar irradiance, clear-sky index, Poisson process, stochastic differential equations.

I. INTRODUCTION

A. Motivation

With an installed capacity that has doubled in the last three years, solar Photovoltaic (PV) generation is the fastest growing energy source in power systems worldwide [1]. Solar generation is renewable and eco-friendly but also highly volatile due to the position of the sun and clouds changing [2]. The impact of solar generation fluctuations on the dynamic behavior of power systems has not been thoroughly investigated and remains a relevant research question. Accurate models are required to represent the solar irradiance fluctuations in power system simulations. This paper addresses this modeling need.

B. Literature Review

The output of PV solar power plants naturally changes throughout the day because of the daily path the sun follows across the sky. During sunrise and sunset the output of the PV plant will change by about 10% in just 15 min. The daily sun path can be easily and accurately predicted. On the other hand, PV power plants are also a significant source of intermittency due to cloud coverage. The change in solar irradiance caused by cloud movement can be over 60% of the peak irradiance within a few seconds [3]. These variations can be smoothed and their transient effects minimized if considering a large PV power plant or an aggregated model of several geographically distributed plants [2]. However, if a single PV power plant covers a relatively small area, e.g., in microgrid applications, its power output fluctuations have to be properly modelled [4].

Based on the discussion above, solar irradiance variations can be divided into a deterministic component and a stochastic one. The deterministic component is the variations at a minutely or hourly scale due to the daily apparent movement

of the sun. This trajectory can be accurately predicted based on location, time of year and day using clear-sky irradiance models [5], [6]. The stochastic variability is dependent on the cloud coverage and can be expressed using the clear-sky index (the ratio between the global solar radiation and the corresponding clear-sky radiation).

In the dynamic analysis of power systems with PV generation, the solar irradiance is either assumed to be constant [7], [8] or to vary with random steps [9]–[11]. These models do not capture the actual intermittency of the solar irradiance. Measurement data has to be utilized to build more accurate models.

In [12], the solar irradiance variability is modeled by combining a Poisson jump process and an Autoregressive Moving Average (ARMA) model. Stochastic Differential Equations (SDEs) with jumps are defined in [4] for modeling the clear-sky index. Both these methods define model parameters based on measurements. However, these models do not adequately capture the volatility of the solar irradiance in the seconds to minutes time scale.

C. Contributions

The contributions of this paper are twofold.

- To describe three models of solar irradiance volatility previously presented in [10], [12], and [4], respectively, and discuss the shortcomings of such models.
- To propose a novel model of the clear-sky index for short-term dynamic analysis.

In the proposed model, clear-sky conditions are represented through a SDE and the jumps caused by cloud movements are simulated with two jump diffusion processes. The paper also shows how the proposed approach overcomes the issues of the other models.

D. Organization

The reminder of this work is organized as follows. Section II describes the solar irradiance measurement data utilized throughout the paper and outlines the modeling of solar irradiance. Section III presents four solar irradiance models and Section IV shows how the proposed model can be used to generate synthetic solar irradiance processes that accurately capture the intermittent behaviour of real-world data. Finally, Section V draws conclusions and outlines relevant areas for future work.

II. MODELING OF SOLAR IRRADIANCE

This section presents the procedure to identify the deterministic and stochastic part of the solar irradiance from measurement data. With this aim and for further analysis in the paper, the solar irradiance data collected by the National Renewable Energy Laboratory (NREL), gathered in Kalaeloa, Hawaii, are used [13]. This data set consists of one year of measurements gathered with a 1 Hz sampling frequency from April 2010 to March 2011. Each day consists of measurements from 5am to 8pm.

Irradiance is a measure of the power of sunlight (W/m^2). The power output of a PV panel is proportional to the solar irradiance that hits the panel. Figure 1 shows the solar irradiance measurements over three whole days, with different clouding conditions. The effective Global Horizontal Irradiance (GHI) on the solar panel can be modeled in two parts. The deterministic part, which is the estimated clear-sky irradiance based on the position of the sun and the stochastic part, dependent on the cloud movement.

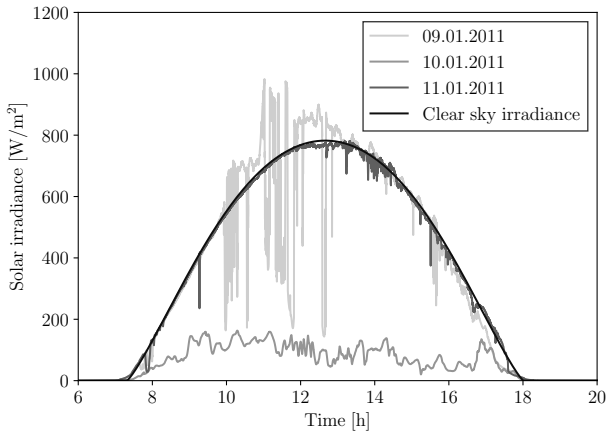


Fig. 1. Measured solar irradiance [13] and estimated clear-sky global solar irradiance using (2).

The temporal variability of solar irradiance, due to cloud coverage, can be modeled through the clear-sky index, k . This is defined as the ratio between the measured GHI, G , and the estimated global horizontal clear-sky irradiance, G_C :

$$k = \frac{G}{G_C}. \quad (1)$$

The clear-sky index for the three days in Fig. 1 is shown in Fig. 2.

The clear-sky global solar irradiance is the maximum irradiance arriving at earth's surface at a specific location and time, i.e., when no clouds are present. The clear-sky irradiance depends on the site, the solar elevation angle and various atmospheric conditions [6].

A number of models of varying complexity have been suggested in the literature to model the clear-sky irradiance. In this paper, a clear-sky model of the same form as the Adnot-Bourges-Campana-Gicquel model is used [5]:

$$G_C = a \cdot \cos(z)^b, \quad (2)$$

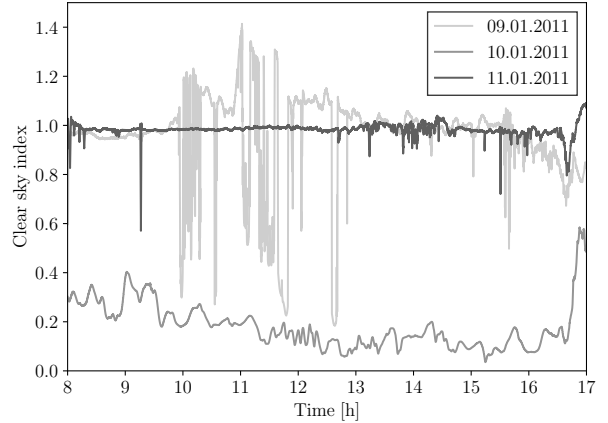


Fig. 2. Clear-sky index found for the measured solar irradiance data shown in Fig. 1. In some cases, the clear-sky index becomes bigger than zero during flickering conditions. This is due to cloud enhancement, i.e., sunlight being reflected by surrounding clouds.

where z is the zenith angle, which is estimated based on the location and time of day. The parameters a and b are determined by fitting equation (2) to the measured data for clear-sky days [6]. These coefficients change day by day and are thus found for each clear day of the data set. For the remaining days, a and b coefficients are estimated based on the parameters for the clear days.

The data sets of clear-sky indexes for one day are limited by the sunrise and sunset, that is when $G_C(t) > 0$. The low values of GHI occurring just after sunrise and sunset result in higher uncertainties in the clear-sky index [14]. Because of this, only solar irradiance data from 8am to 5pm are used.

III. MODELS OF THE CLEAR-SKY INDEX

This section presents four models to model the fluctuations of the clear-sky index. The first three models have been presented in the literature to represent solar irradiance fluctuations for the short-term (seconds-to-minutes time scale) analysis of power systems. The fourth model, which is proposed in this paper, addresses the shortcomings of the available models and proposes a novel way to reproduce the jumps in the clear-sky index.

A. Model I

This model is a simple way to represent the clear-sky index variations in simulation [10], [11]. Such variations are represented by a random signal between 1 and 0.4, with 5 second steps. Figure 3 shows an example of a simulated clear-sky index obtained with Model I. The range of the jump size and the waiting time between jumps can be changed to fit different locations. However, it is not possible to vary the waiting time between consecutive jumps or to consider the correlation of jump amplitudes.

B. Model II

This model, presented in [12], as well as the following two models, split the representation of the clear-sky index into two

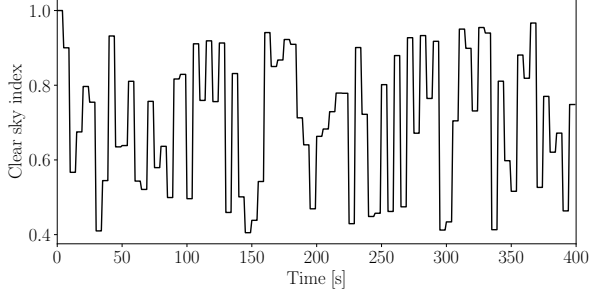


Fig. 3. Clear-sky index generated with Model I.

parts:

1. The baseline of the clear-sky index varying around 1, which models the clear-sky condition.
2. The jumps of the clear-sky index due to cloud coverage.

The baseline is modeled using an Autoregressive Moving Average (ARMA) model. ARMA models are discrete, with a fixed time step that must match the sampling interval of the data. Measured solar irradiance data sampled every minute is used to define the parameters of the model. In [12], interpolation is used to convert the model from a time-step of one minute to one second.

The number of cloud events E (jumps) are modeled using a Poisson random variable, with the mean λ and the probability density function:

$$f(x, \lambda) = \frac{\lambda^x}{x!} \exp(-\lambda), \quad (3)$$

where $x = 0, 1, 2, \dots$. The inter-event waiting time, i.e., the time between cloud events, is itself a random variable with an exponential distribution with mean μ_W :

$$f_W(t) = \frac{1}{\mu_W} \exp(-t/\mu_W), \quad (4)$$

where $t \geq 0$. Finally, the duration T_D of a cloud event is assumed to be exponentially distributed with mean μ_D . A detailed description of how the parameters for the cloud events are derived can be found in [12].

In the following, the ARMA model is substituted with an Ornstein-Uhlenbeck Stochastic Differential Equation (SDE) to illustrate the properties of this model. This substitution has no side effect as the variations of the baseline are minimal in the considered time scale. The SDE is defined as:

$$dX(t) = \theta(\mu - X(t))dt + \sigma dW(t), \quad (5)$$

where $\mu, \theta > 0$ and $\sigma > 0$ are parameters and $W(t)$ is a Wiener process. The process described by (5) is a continuous-time equivalent of an ARMA(1,0) process. Models III and IV, which are discussed below, also utilize the process in (5) to represent the stochastic clear-sky conditions.

Figure 4 shows an example of a simulated clear-sky index, generated with Model II and with the parameters of the jump process that represent the spring data set, i.e., $\lambda = 7.4178$, $\mu_W = 46.5186$ and $\mu_D = 54.0616$ [12]. In this model, the jump amplitude is the same for all cloud events, which is not realistic.

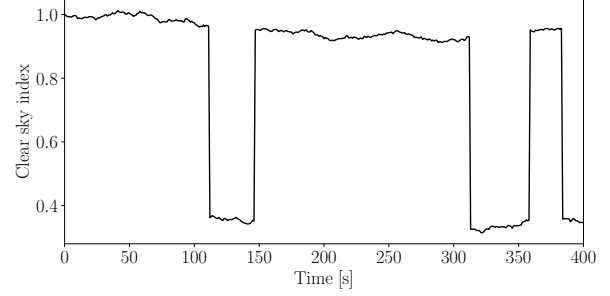


Fig. 4. Clear-sky index generated with Model II.

C. Model III

This model was presented in [4] and uses jump diffusion processes, i.e., SDEs with jumps, to represent the clear-sky index. A general jump diffusion process is defined as:

$$dY(t) = a(Y(t), t) + b(Y(t), t)dW(t) + \xi dJ(t), \quad (6)$$

where $a(Y(t), t)$ and $b(Y(t), t)$ are the drift and diffusion terms, respectively; ξ is a jump size that is assumed to be a normally distributed random number, $\xi \sim N(\mu_\xi, \sigma_\xi)$; and $J(t)$ is a Poisson process with jump rate λ , as defined in (3). In the following, for comparison, it is assumed that the first two terms on the right-hand side of (6) represent an Ornstein-Uhlenbeck process, as in (5).

In [4], three scenarios are modeled: cloudy, flickering and sunny. For the cloudy and sunny scenarios, no jumps are considered ($\xi = 0$). Then, a non-parametric estimation method is used for estimating the parameters of the model. Figure 5 shows an example of a simulated clear-sky index in the flickering state obtained with Model III. The parameters defined in [4] for the flickering state are used, namely, $\lambda = 0.01$, $\sigma_\xi = 0.028$ and $\mu_\xi = 0.7$. The number of times the clear-sky index data crosses its mean value (~ 0.7) is used for defining the jump rate λ . This assumption clearly prevents modeling any jump that is smaller than the threshold defined by the mean value.

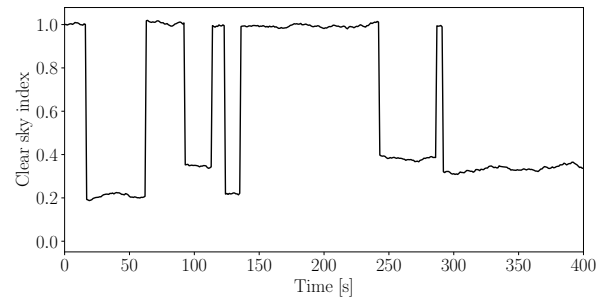


Fig. 5. Clear-sky index generated with Model III.

D. Model IV (Proposed Model)

If the clear-sky indexes generated using Models I to III above are compared with measurement data, two limitations

become apparent. Firstly, they are based on the whole data set, not on the flickering cloudy conditions solely. For this reason, these models cannot capture the dynamics of fast variations in the time scale of seconds to minutes. Secondly, small jumps of the clear-sky index are neglected.

The model proposed in this section is aimed at capturing clear-sky index variations for flickering clouding events over the time scale of seconds to minutes. The proposed method utilizes the Ornstein-Uhlenbeck SDE in (5) to represent the clear-sky stochastic variations in the same way as is done in Method II and III. Since the jumps do not depend on the stochastic variable $X(t)$ and are additive noise (see (6)), they are added directly to the $X(t)$, thus simplifying the numerical integration. The interested reader can find the detailed procedure to integrate jump diffusion processes in [15].

The jumps are modeled as:

$$H(t) = mP(t), \quad (7)$$

where m is the jump amplitude assumed to be a normally distributed random number, namely, $m \sim N(\mu_m, \sigma_m^2)$. $P(t)$ is a step function that can get only 0/1 values, where the number of transitions per period are determined with Poisson distribution with parameter λ as in (3). The duration of each jump is determined with a normal distribution $\delta \sim N(0, \sigma_\delta^2)$. In turn, each time $P(t)$ switches from 0 to 1 (or to 1 to 0), it remains constant for a time δ .

Visual inspection of the measured clear-sky index data allows identifying two types of jumps of the clear-sky index:

- **Jump model 1 (JM1):** Big clouds passing over the PV that block most of the solar irradiance.
- **Jump model 2 (JM2):** Small clouds that typically pass by more frequently and only partially reduce the solar irradiance.

The resulting proposed model of the clear-sky index is:

$$k(t) = X(t) + u(t)G(t), \quad (8)$$

where $X(t)$ is defined by (5) and $u(t)$ is a function that defines the duration of a clouding event:

$$u(t) = \begin{cases} 1 & \text{if } u_{start} \leq t \leq u_{stop} \\ 0 & \text{otherwise,} \end{cases} \quad (9)$$

where u_{start} and u_{stop} are the starting and ending times of the clouding event and

$$G(t) = \begin{cases} -H_1(t) + H_2(t) & \text{if } H_1(t) > 0 \\ -H_2(t) & \text{otherwise,} \end{cases} \quad (10)$$

where $H_1(t)$ and $H_2(t)$ are JM1 and JM2, respectively.

The data set presented in Section II is used for evaluating the parameters of the jump models. Five clouding events for each month, for a total of 60 events, are analyzed. This analysis leads to the parameters shown in Table I. These parameters are utilised in the remainder of the paper to represent the jumps of the clear-sky index for Model IV, as discussed in the following section.

TABLE I
RANGE OF PARAMETERS FOR THE JUMP MODELS OF MODEL IV DEFINED BASED ON THE ANALYSIS OF 60 CLOUDING EVENTS

Parameters	Jump model 1	Jump model 2
λ	0.005 – 0.05	0.05 – 0.1
μ_m	0.6 – 0.8	0
σ_m^2	0.0005 – 0.005	0.01 – 0.1
σ_δ^2	10 – 50	1 – 5

TABLE II
PARAMETERS OF MODEL IV FOR THE CLOUDING EVENT SHOWN IN FIG. 6

Parameters	Jump model 1	Jump model 2
λ	0.007	0.05
μ_m	0.7	0
σ_m^2	30	3
σ_δ^2	0.05	0.001

IV. CASE STUDY

A cloud event from the data set presented in Section II is considered in this section to illustrate Model IV and compare its output with Models I to III discussed above. The event occurred on the 1st of December 2010 and its duration was 450 s. The analysis of the behavior of the clear-sky index during this event allows determining the parameters for the clear-sky index through Model IV.

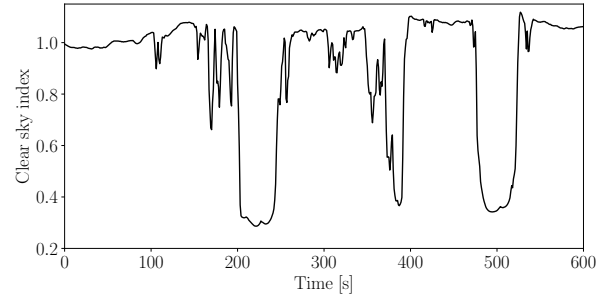


Fig. 6. Clear-sky index obtained from measurement data [13] and clear-sky model (2).

The first step is to identify the parameters for JM1. Three periods of low clear-sky indexes can be clearly seen from Fig. 6. From this values, one obtains that the number of jumps in the unit of time (450 s), is $3/450 = 0.007$. This value is within the range given in Table I and, just for the sake of example, the Poisson distribution parameter is set $\lambda = 0.007$. With similar assumptions, the average and variance of the jumps amplitudes are set to $\mu_m = 0.7$ and $\sigma_m^2 = 0.001$, respectively, whereas the variance that defines the distribution of the duration of big clouding events is set to $\sigma_\delta^2 = 30$.

The second step is to identify the parameters for JM2. Only jumps in the measured clear-sky index that exceed 0.1 are considered. Such a number is found to be 23 and, hence, $\lambda = 23/450 \approx 0.05$ is used. The remaining parameters for JM2 are identified in the same way as the parameters for JM1. All parameters of Model IV for the clouding event in Fig. 6 are shown in Table II.

Using Model IV and the parameters of Table II, one can generate synthetic scenarios that are comparable with the

measurement data clouding event shown in Fig. 6. Two sample processes are shown in Fig. 7. Visual inspection reveals that the proposed model is able to reproduce the main features of the clouding event of the measurement data in the time-domain.

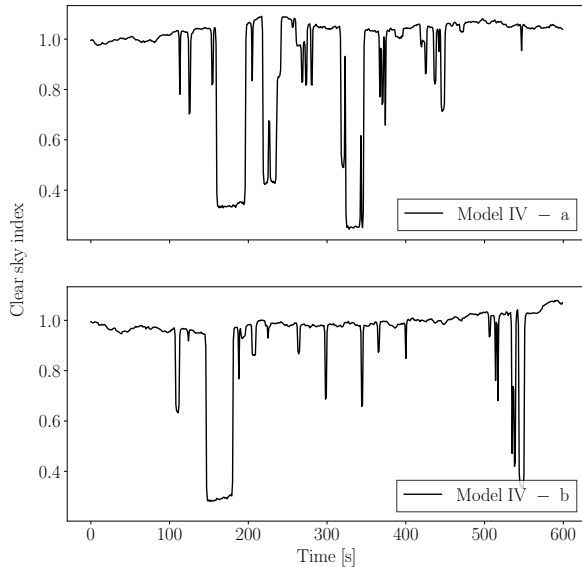


Fig. 7. Two sample synthetic clear-sky index processes, generated with Model IV and based on the cloud event shown in Fig. 6.

Figure 8 compares the probability distributions of the measured and simulated clear-sky indexes. Model I does not capture the two peaks in the probability distribution, while Models II and III capture the peaks but not the distribution between the peaks. Model IV is able to better reproduce the clear-sky indexes probability distribution and time-domain behavior when compared to Models I-III.

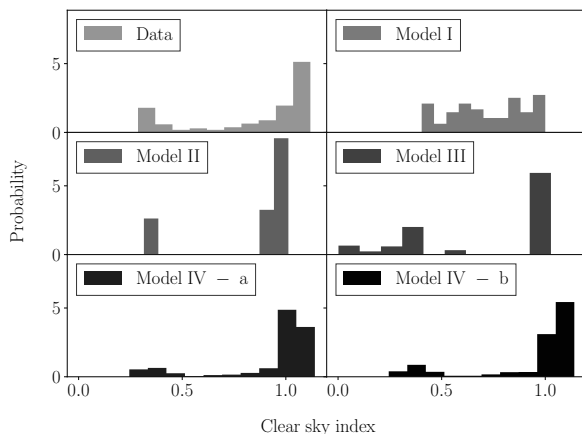


Fig. 8. Histograms of the clear-sky index during the clouding event shown in Fig. 6 and the generated clear-sky indexes obtained with Models I-IV.

V. CONCLUSIONS

This paper deals with the modeling of solar irradiance for short-term analysis of PV solar generation. Three models previously proposed in the literature are discussed. It is concluded that these models do not fully capture the behavior of big jumps of the solar irradiance and fail to model small jumps.

To cope with these issues, a novel model is proposed in the paper based on measurement data. The model considers individual cloudy flickering events. Jumps are grouped considering two thresholds. In this way, the proposed model is able to capture both big jumps, caused by full cloud coverage, and small jumps, due to partial blockage of the sun. Finally, it is demonstrated how synthetic data can be generated to replicate the actual behavior of an individual clouding event, as observed in real-world measurements.

Future work will focus on studying the impact of the flickering of the solar irradiance in power system models. This is done by including the proposed solar irradiance model in power system models with PV solar power plants.

REFERENCES

- [1] BP, Statistical Review of World Energy (June 2018). [Online]. Available: <https://www.bp.com/en/global/corporate/energy-economics/statistical-review-of-world-energy/renewable-energy/solar-energy.html>
- [2] A. Mills, M. Ahlstrom, M. Brower, A. Ellis, R. George, T. Hoff, B. Kroposki, C. Lenox, N. Miller, M. Milligan, *et al.*, “Dark shadows,” *Power and Energy Magazine*, vol. 9, no. 3, pp. 33–41, 2011.
- [3] A. Mills, M. Ahlstrom, M. Brower, A. Ellis, R. George, T. Hoff, B. Kroposki, C. Lenox, N. Miller, J. Stein, *et al.*, “Understanding variability and uncertainty of photovoltaics for integration with the electric power system,” *The Electricity Journal*, 2009.
- [4] M. Anvari, B. Werther, G. Lohmann, M. Wächter, J. Peinke, and H.-P. Beck, “Suppressing power output fluctuations of photovoltaic power plants,” *Solar Energy*, vol. 157, pp. 735–743, 2017.
- [5] Y. Dazhi, P. Jirutitijaroen, and W. M. Walsh, “The estimation of clear sky global horizontal irradiance at the equator,” *Energy Procedia*, vol. 25, pp. 141–148, 2012.
- [6] M. J. Reno, C. W. Hansen, and J. S. Stein, “Global horizontal irradiance clear sky models: Implementation and analysis,” *Sandia report (SAND2012-2389)*, 2012.
- [7] R. Elliott, A. Ellis, P. Pourbeik, J. Sanchez-Gasca, J. Senthil, and J. Weber, “Generic photovoltaic system models for WECC-a status report,” in *Power & Energy Society General Meeting, IEEE*, 2015.
- [8] M. Hossain, T. Saha, N. Mithulanathan, and H. Pota, “Robust control strategy for PV system integration in distribution systems,” *Applied Energy*, vol. 99, pp. 355–362, 2012.
- [9] T. Alquthami, H. Ravindra, M. Faruque, M. Steurer, and T. Baldwin, “Study of photovoltaic integration impact on system stability using custom model of PV arrays integrated with PSS/E,” in *North American Power Symposium (NAPS)*. IEEE, 2010, pp. 1–8.
- [10] R. Ayyanar and A. Nagarajan, “Distribution system analysis tools for studying high penetration of PV with grid support features,” *Arizona State University, Tech. Rep.*, 2013.
- [11] A. Nagarajan and R. Ayyanar, “Methods for dynamic analysis of distribution feeders with high penetration of PV generators,” in *Photovoltaic Specialists Conference (PVSC), IEEE*, 2016, pp. 1848–1852.
- [12] J. Sexauer and S. Mohagheghi, “Hybrid stochastic short-term models for wind and solar energy trajectories,” in *Green Technologies Conference (GreenTech), 2015 Seventh Annual IEEE*, 2015, pp. 191–198.
- [13] M. Sengupta, A. Andreas (2010). Oahu Solar Measurement Grid (1-Year Archive): 1-Second Solar Irradiance; Oahu, Hawaii (Data); NREL Report No. DA-5500-56506. [Online]. Available: <http://dx.doi.org/10.5439/1052451>
- [14] M. Lave, J. Kleissl, and E. Arias-Castro, “High-frequency irradiance fluctuations and geographic smoothing,” *Solar Energy*, vol. 86, no. 8, pp. 2190–2199, 2012.
- [15] E. Platen and N. Bruti-Liberati, *Numerical Solution of Stochastic Differential Equations with Jumps in Finance*. Berlin Heidelberg: Springer - Verlag, 2010.